JACS
JOURNAL OF THE AMERICAN CHEMICAL SOCIETY
Article
pubs.acs.org/JACS

Extended String Binding Mode of the Phosphorylated Transactivation Domain of Tumor Suppressor p53

Masahiko Okuda and Yoshifumi Nishimura*

Graduate School of Medical Life Science, Yokohama City University, 1-7-29 Suehiro-cho, Tsurumi-ku, Yokohama 230-0045, Japan

Supporting Information

ABSTRACT: The transactivation domain (TAD) of tumor suppressor p53 has homologous subdomains, TAD1 and TAD2. Both are intrinsically disordered in their free states, but all structures of TAD1 and TAD2 bound to their target proteins have demonstrated use of an amphipathic α-helix, suggesting that the binding-coupled helix folding mechanism of TAD1 and TAD2 is essential. Although phosphorylation of TAD is important to switch the function of p53, bound structures of phosphorylated TAD1 and TAD2 have not been determined. Here, we reveal the recognition mechanism of the phosphorylated TAD2 bound to a pleckstrin homology (PH) domain from human TFIIH subunit p62 in an extended string-like conformation. This string-like binding mode of TAD2 seems to be independent of its phosphorylation in spite of enhanced binding activity upon phosphorylation. This is in contrast to the amphipathic helical binding mode of the unphosphorylated TAD2 to the yeast tfb1 PH domain and demonstrates that the p53 TAD2 has much higher conformational malleability than previously appreciated.

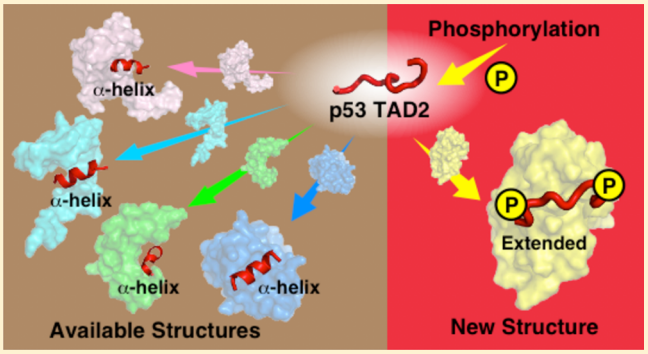

INTRODUCTION

The p53 tumor suppressor is a key protein of the cellular stress response, having roles in DNA repair, cell cycle arrest, apoptosis, senescence, metabolism, and autophagy.[1−4] The N-terminus of p53 is the acidic transactivation domain (TAD, residues 1−61) and is important for p53 transcription activity through the interaction with transcription factors, including transcription co-activators, co-repressors, and the general transcription factors TFIID and TFIIH. The TAD contains two homologous subdomains, TAD1 (residues 1−42) and TAD2 (residues 43−61), containing a conserved ΦXXΦΦ motif (Φ = a bulky hydrophobic residue, X = any other residue), and both function as hub domains, contacting multiple partners in complicated protein−protein networks of p53. Although the TAD is largely unstructured in a target-free state, local structural elements, namely an amphipathic helix in the TAD1 (residues 18−26) and two turns in the TAD2 (residues 40−44, 48−53), are transiently formed.[5] Both regions are interacting regions for various target proteins, and so far tertiary structures of four TAD1 and four TAD2 complexes bound to their targets have been determined: TAD1 bound to the ubiquitin E3 ligase, MDM2;[6] the homologue of MDM2, MDMX;[7] and the co-activators p300[8] and CREB binding protein (CBP);[9] and TAD2 bound to the replication protein A;[10] the yeast general transcription factor tfb1;[11] CBP,[9] and high-mobility group B1 protein.[12] Structural models of complexes of TAD2 bound to the positive co-factor 4,[13] and the anti-apoptotic Bcl-2 family proteins, Bcl-2 and Bcl-X_L,[14] have also been proposed on the basis of NMR experiments.

It is noteworthy that in all of the complexes thus far available, TAD1 and TAD2 form an amphipathic α-helix on their target proteins. From these results, binding-coupled amphipathic α-helix formation has been understood to be an essential binding mode of TAD1 and TAD2 in their target recognition. In fact, several small molecules and high-affinity peptides that inhibit the interaction of TAD1 with MDM2 and MDMX have been designed as anticancer drugs based on these α-helical complex structures.[15−19]

The TAD2 of human p53 specifically binds to a pleckstrin homology (PH) domain of human TFIIH subunit p62.[20] p62 is also an important hub protein which links transcription and DNA repair processes. Besides p53, p62 interacts with the general transcription factor, TFIIEα,[21,22] and the transcriptional activators, E2F1,[23] estrogen receptor,[24] and erythroid Krüppel-like factor (EKLF).[25] It also binds the viral transactivators, herpes simplex virus protein VP16[20] and Epstein−Barr virus nuclear antigen 2,[26] the nucleotide excision repair factors XPC/HR23B[27] and XPG,[28] and the papilloma virus E1 helicase, which is essential for initiation of viral DNA replication.[29] To date, due to the low solubility and stability of the p62 PH domain, the tertiary complex structure of the human p62 PH domain was only available in a complex with an acidic domain of TFIIEα (that we previously solved by NMR[22]).

Although no homologue of p53 has been identified in yeast cells, it is interesting to note that human p53 was revealed to

Received: June 24, 2014
Published: September 12, 2014

   dx.doi.org/10.1021/ja506351f | J. Am. Chem. Soc. 2014, 136, 14143−14152

bind to the budding yeast tfb1, a homologue of human TFIIH p62, and the tertiary structure of the complex between human p53 TAD2 and the yeast tfb1 PH domain was determined.[11] In addition, five tertiary structures of complexes involving the yeast tfb1 PH domain have been solved.[25,30−33] Although the human p53 TAD2 was reported to interact with the corresponding surface of the human p62 PH domain, as found in the complex with the yeast tfb1 PH domain by NMR titration experiment, the tertiary structure of the p53 TAD2 bound to the human p62 PH domain was not determined in these studies.[11,34]

In protein−protein networks of p53, phosphorylation serves as an essential regulatory switch. In unstressed cells, p53 is maintained at low levels primarily by its negative regulator MDM2. In response to cellular stresses such as DNA damage and oncogene activation, p53 is stabilized by phosphorylation and other post-translational modifications, accumulates in the nucleus, and selectively activates subsets of genes involved in cell cycle arrest, apoptosis, senescence, metabolism, or autophagy depending on the kind and the extent of stresses.[35,36] Human p53 has seven serine and two threonine residues (Ser6, 9, 15, 20, 33, 37, 46 and Thr18, 55) in the TAD, whose phosphorylation has been implicated in p53 activation upon stresses.[37] For example, the phosphorylation of Thr18 weakens the interaction between TAD1 and the negative regulator MDM2, leading to the increase of stabilization of p53 and its transcriptional activity.[38] Phosphorylation of other sites (Ser15, 20, 33, 37, 46 and Thr55) in addition to Thr18 further decreases this interaction.[39] In contrast, phosphorylation of each of these seven residues enhances the affinity for the four p53 TAD-binding domains (TAZ1, KIX, TAZ2, and NCBD) of the co-activators p300 and CBP to varying degrees.[39−42] Ser6 and Ser9 are phosphorylated in response to various genotoxic and nongenotoxic stresses.[43,44] The phosphorylation of Ser46 regulates p53 apoptotic activity.[45,46] The phosphorylation at Thr55 is involved in G1 cell cycle progression via the degradation of p53[47] and in nuclear export of p53.[48] Phosphorylation of Ser46 and Thr55 increases the affinity for PH domains of human p62 and yeast tfb1.[11] The functional roles of phosphorylation of p53 have been extensively studied, but the tertiary structures of complexed phosphorylated TAD1 or TAD2 have not yet been determined.

In this study, we have determined the tertiary structure of the Ser46 and Thr55-phosphorylated p53 TAD2 bound to the PH domain of TFIIH p62. Although the unphosphorylated TAD2 has been shown to form an amphipathic helix in the bound form on the target proteins thus far examined as described above, remarkably the structure presented here of the phosphorylated TAD2 is an extended string-like structure. Such a string structure formation is independent of the phosphorylation, whereas the binding activity is significantly augmented in a phosphorylation-dependent manner. Together with the results of the complex structure and the mutational analyses by ITC and NMR, we identify the structural determinants for the malleable and specific binding of p53 and explain why TAD2 adopts the elongated string-like conformation on the human p62 PH domain and not an amphipathic helix.

EXPERIMENTAL PROCEDURES

Preparation of Human TFIIH p62 PH Domain. Unlabeled, ^{15}N-labeled, and ^{13}C/^{15}N-labeled human TFIIH p62 PH domain (residues 1−108) were prepared as previously described.[22] Briefly, they were expressed as glutathione S-transferase (GST)-fused products in pGEX-4T vectors (GE Healthcare) in *E. coli* BL21(DE3) (Merck Millipore). Lysed supernatant was loaded onto a glutathione Sepharose (GE Healthcare) column. The eluate was then digested with thrombin to remove the GST. After concentration using an Amicon Ultra device (Merck Millipore), the sample was applied onto a Superdex75 column (GE Healthcare).

Preparation of Human p53 TAD2 Peptides. Unphosphorylated and Ser46-, Thr55-, and Ser46,Thr55-phosphorylated peptides of human p53 TAD2 (residues 41−62) were purchased from Sigma Genosys.

Preparation of Human p53 TAD. The ^{13}C/^{15}N-labeled human p53 TAD (residues 1−73) was expressed as a hexa histidine-tagged product in pET11d vectors (Merck Millipore) transformed into *E. coli* Rosetta (DE3) (Merck Millipore). The cells were grown at 37 °C in M9 minimal medium containing [^{15}N]ammonium chloride and [^{13}C]glucose. After 1 mM isopropyl-β-D-thiogalactopyranoside (IPTG) induction and 6 h growth, the cells were harvested. The cell pellet was resuspended in buffer A (20 mM Tris-HCl (pH 8.0), 10% glycerol, 1 M NaCl). The cells were lysed by sonication, centrifuged, and the supernatant loaded onto a Ni-nitrilotriacetic acid (NTA)−agarose (Qiagen) column, equilibrated with buffer A containing 20 mM imidazole-HCl. The sample was eluted by 500 mM imidazole-HCl. Peak fractions were pooled and digested with thrombin for 16 h at 25 °C to remove the histidine tag. The sample was concentrated using Amicon Ultra devices (Merck Millipore) and applied onto a Superdex 30 (GE Healthcare) column equilibrated with 20 mM potassium phosphate (pH 6.8), 500 mM NaCl. Peak fractions were again loaded onto the Ni-NTA agarose column and the sample which passed through the column was concentrated using Amicon Ultra devices.

NMR Spectroscopy. The Ser46,Thr55-phosphorylated p53 TAD2 peptide in 20 mM potassium phosphate (pH 6.8), 5 mM deuterated DTT, and either 10% D_2O or 99.9% D_2O was added to 0.4−0.5 mM of ^{13}C/^{15}N-labeled TFIIH p62 PH domain in the same buffer at a molar ratio of 1.0:1.2 to prepare the complex. NMR experiments were performed at 32 °C on Bruker AVANCE-600 and AVANCE-800 spectrometers, each equipped with a cryogenic probe. Backbone and side chain resonances for p62 PH domain were assigned using standard triple-resonance NMR experiments.[49] Stereospecific assignments for p62 PH domain were obtained from a combination of HNHB, HN(CO)HB, HNCG, HN(CO)CG, and ^{13}C-edited NOESY-HSQC (τ_m = 50 ms). The p53 phosphorylated TAD2 peptide resonances were assigned using ^{13}C, ^{15}N-filtered TOCSY and NOESY experiments. All resonances, except for the backbone amide protons of Asp42, Phe54, and Thr55, were assigned (Supporting Information, Table S1). Intramolecular distance restraints were obtained from ^{15}N-edited NOESY-HSQC (τ_m = 50 and 150 ms) and ^{13}C-edited NOESY-HSQC (τ_m = 50 and 100 ms) for p62 PH domain, and ^{13}C, ^{15}N-filtered NOESY for p53 phosphorylated TAD2 peptide. Intermolecular distance restraints were obtained from ^{13}C, ^{15}N filtered/edited NOESY (τ_m = 120 and 150 ms). Side-chain torsion angles, χ_1 and χ_2 were obtained from a combination of HNHB, HN(CO)HB, HNCG, HN(CO)CG, and ^{13}C-edited NOESY-HSQC (τ_m = 50 ms). Hydrogen bond restraints were obtained by backbone amide H/D-exchange experiments. The ^{13}C/^{15}N-labeled, unphosphorylated p53 TAD in 20 mM potassium phosphate (pH 6.8), 5 mM deuterated DTT, 10% D_2O was added to 0.3 mM TFIIH p62 PH domain in the same buffer at a molar ratio of 1.2:1.0. NMR experiments were performed at 32 °C on a Bruker AVANCE-600 spectrometer equipped with a cryogenic probe. Backbone resonances for p53 TAD in the unbound and bound forms were assigned using standard triple-resonance NMR experiments.[49] Spectra were processed by NMRPipe[50] and analyzed by NMRView.[51]

Structure Calculation. In total, 171 and 2640 NOE-derived distance restraints were collected for the p53 phosphorylated TAD2 and the TFIIH p62 PH domains, respectively (Supporting Information, Table S2). In addition, 92 hydrogen bond restraints and 248 dihedral angle restraints were collected for the p62 PH domain. For the intermolecular distance restraints, 129 intermolecular

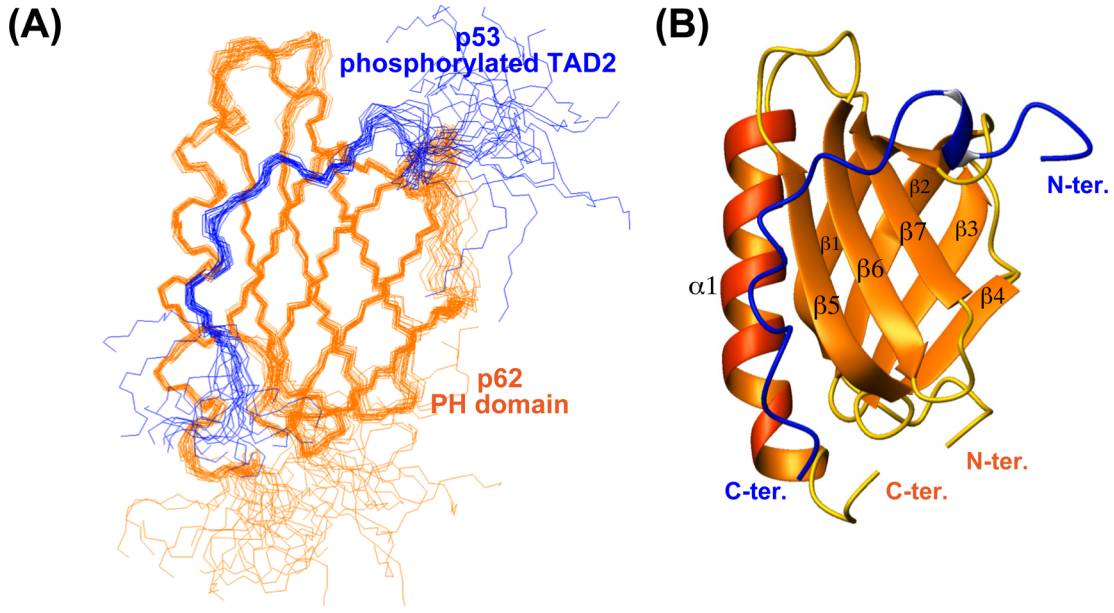

Figure 1. Structures of the p53 phosphorylated TAD2−TFIIH p62 PH domain complex. (A) Overlay of the 20 best structures. (B) The lowest energy structure (see Table S2).

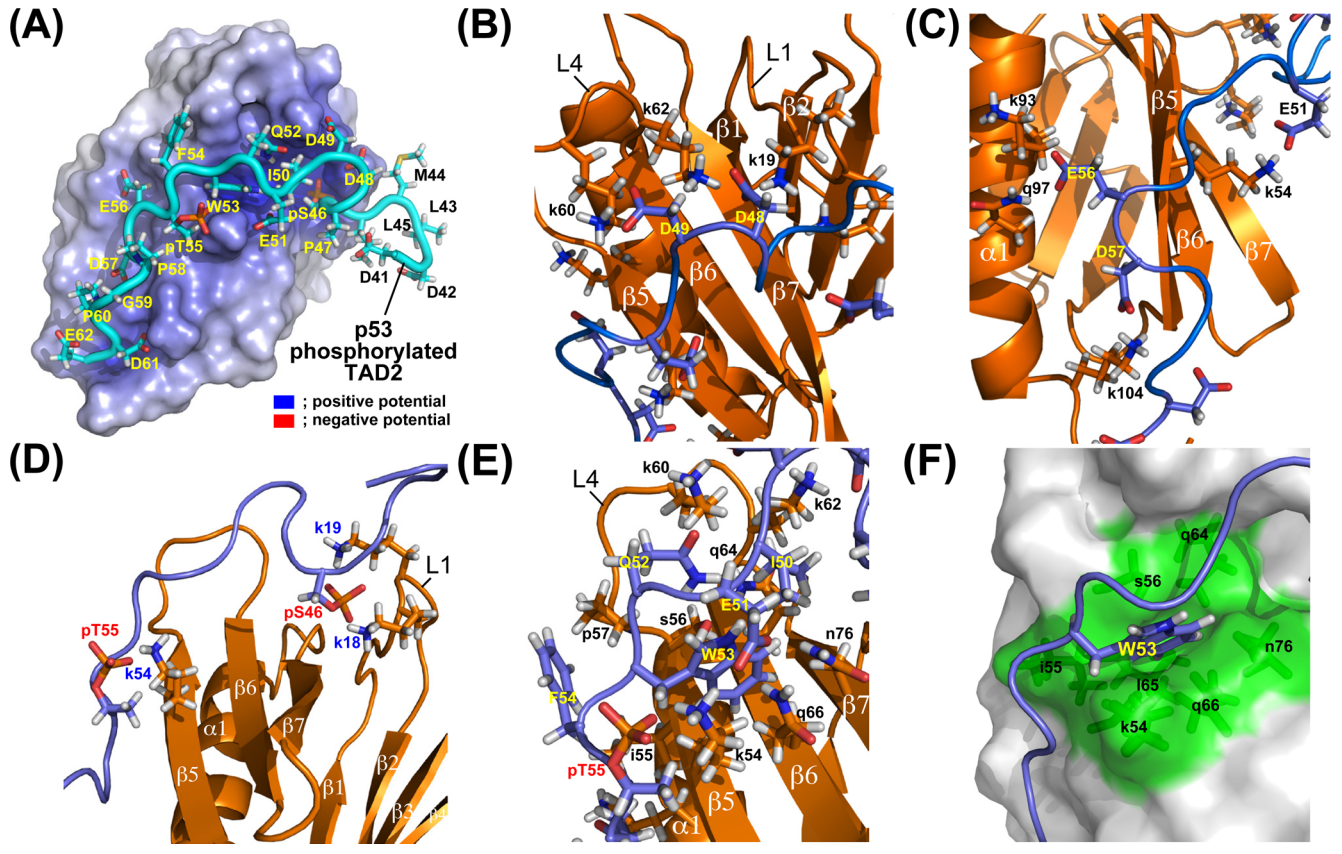

Figure 2. Interactions at the interface. (A) Electrostatic potential surface of p62 PH domain. (B,C) Electrostatic interactions between p53 acidic and p62 basic residues. (D) Interactions between p53 phosphorylated Ser46 (pS46), Thr55 (pT55) and p62 basic residues. (E,F) Interactions in the binding pocket of p62 PH domain. The residues of p53 and p62 are labeled with uppercase and lowercase letters, respectively.

NOEs were collected. Interproton distance restraints derived from NOE intensities were grouped into four distance ranges, 1.8−2.7 Å (1.8−2.9 Å for NOEs involving HN protons), 1.8−3.3 Å (1.8−3.5 Å for NOEs involving HN protons), 1.8−5.0 Å, and 1.8−6.0 Å, corresponding to strong, medium, weak, and very weak NOEs, respectively. The upper limit was corrected for constraints involving methyl groups, aromatic ring protons, and nonstereospecifically assigned methylene protons. Dihedral angle restraints for ϕ and ψ were obtained from analysis of the backbone chemical shifts with TALOS.[52] χ_1 and χ_2 angles were restrained ±30° for three side-chain rotamers. Structure calculations were performed by distance geometry and simulated annealing using the program Xplor-NIH.[53,54] A total of

dx.doi.org/10.1021/ja506351f | J. Am. Chem. Soc. 2014, 136, 14143−14152

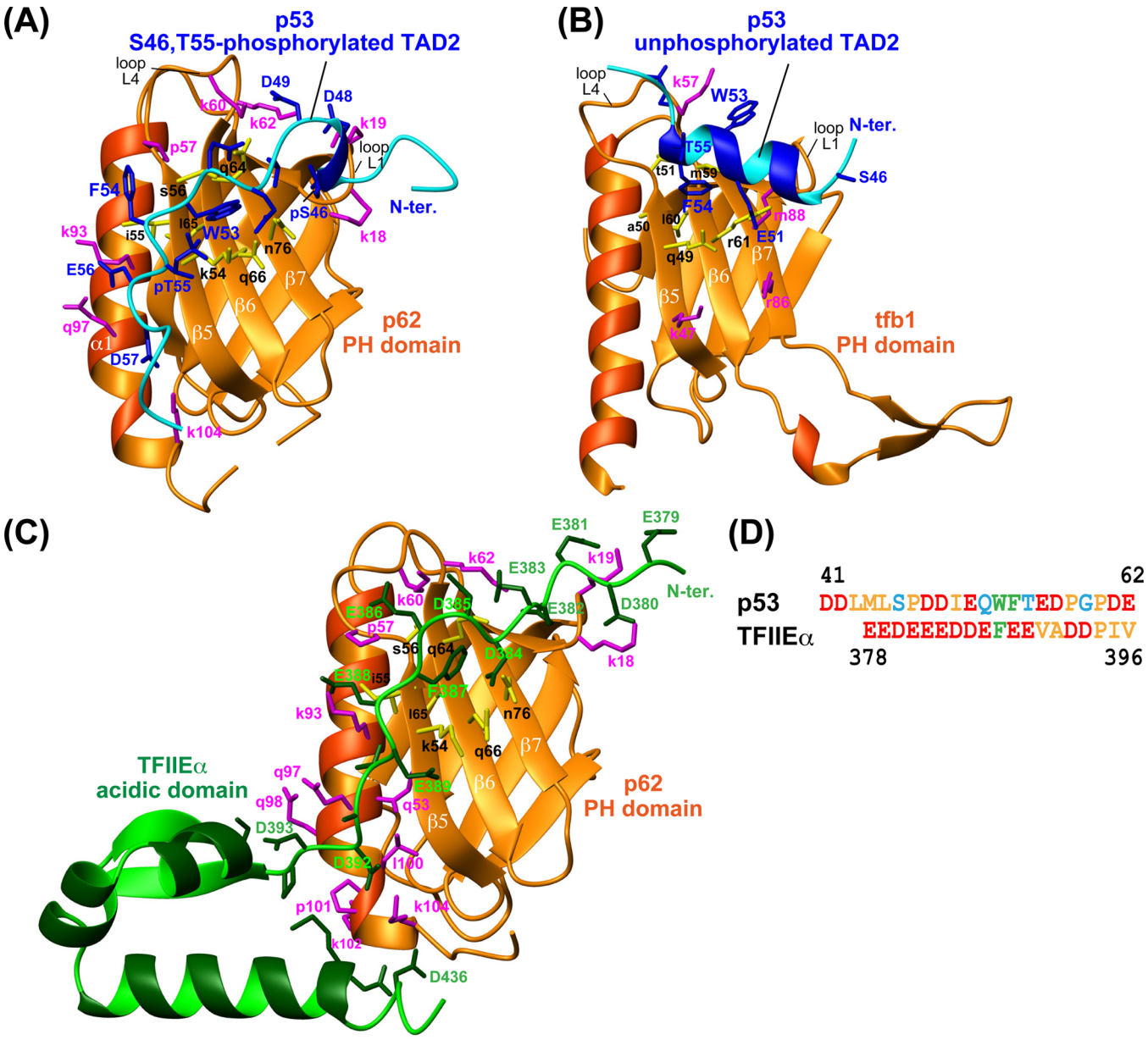

Figure 3. Structure of p53 phosphorylated TAD2−TFIIH p62 PH domain complex and other relevant complexes. (A) p53 phosphorylated TAD2 (blue)/p62 PH domain (orange) complex (PDB code 2RUK). (B) p53 unphosphorylated TAD2 (blue)/yeast tfb1 PH domain (orange) complex (PDB code 2GS0). (C) TFIIEα acidic domain (green)/p62 PH domain (orange) complex (PDB code 2RNR). Binding pockets of p62/tfb1 PH domains are shown in yellow. (D) Alignment of amino acid sequences of the human p53 TAD2 and the N-terminal tail of human TFIIEα acidic domain.

100 structures were calculated. All structures were then subjected to water refinement developed by Linge et al.,[55] in which the structures were immersed in a 7.0 Å layer of water molecules. After minimization with 120 steps, a heating stage from 100 to 500 K with 200 steps of molecular dynamics at every 100 K increment, a refinement stage with 2500 steps at 500 K, and a cooling stage from 500 to 25 K with 200 steps at every 25 K decrement followed. The refinement protocol was finished with 200 steps of minimization. Structural statistics for the 20 best structures are summarized in Table S2. Structures were analyzed and displayed using PROCHECK-NMR,[56] MOLMOL,[57] and PyMOL (DeLano Scientific, San Carlos, CA). The atomic coordinates have been deposited in the Protein Data Bank with accession code: 2RUK.

Isothermal Titration Calorimetry (ITC). The K_d values of p62 PH domain and p53 TAD2 were measured by ITC using a VP-ITC calorimeter (MicroCal). Calorimetric titrations of 300 μM p53 TAD2 in the syringe (25 × 20 μL injections) and 2 mL of 30 μM p62 PH domain in the cell were carried out at 20 °C in 20 mM potassium phosphate (pH 6.8). Each injection took place in 4 s with a preinjection delay of 210 s, and a syringe stirring speed of 307 rpm. Data were analyzed using the Origin software package (MicroCal).

NMR Titration. p53 TAD2 was added to 0.1 mM ^{15}N-labeled p62 PH domain at a molar ratios of 1:0, 1:0.2, 1:0.4, 1:0.6, 1:0.8, 1:1.0, 1:1.2, 1:1.6, 1:2.0, and 1:2.5 (p62 PH:p53 TAD2) in 20 mM potassium phosphate (pH 6.8), 5 mM deuterated DTT dissolved in 10% D_2O. ^{1}H,^{15}N-HSQC spectra were taken before and after p53 TAD2 addition at 32 °C on a Bruker AVANCE-600 spectrometer equipped with a cryogenic probe. Chemical shift change ($\Delta\delta$) was calculated as $\Delta\delta = \{(\Delta\delta^1\mathrm{H})^2 + (\Delta\delta^{15}\mathrm{N}/5)^2\}^{1/2}$.

RESULTS

Overall Structure. The p62 PH domain likely has a rigid, compact structure, showing no significant difference between the free[58] and bound forms. It forms a β-sandwich fold

dx.doi.org/10.1021/ja506351f | J. Am. Chem. Soc. 2014, 136, 14143−14152

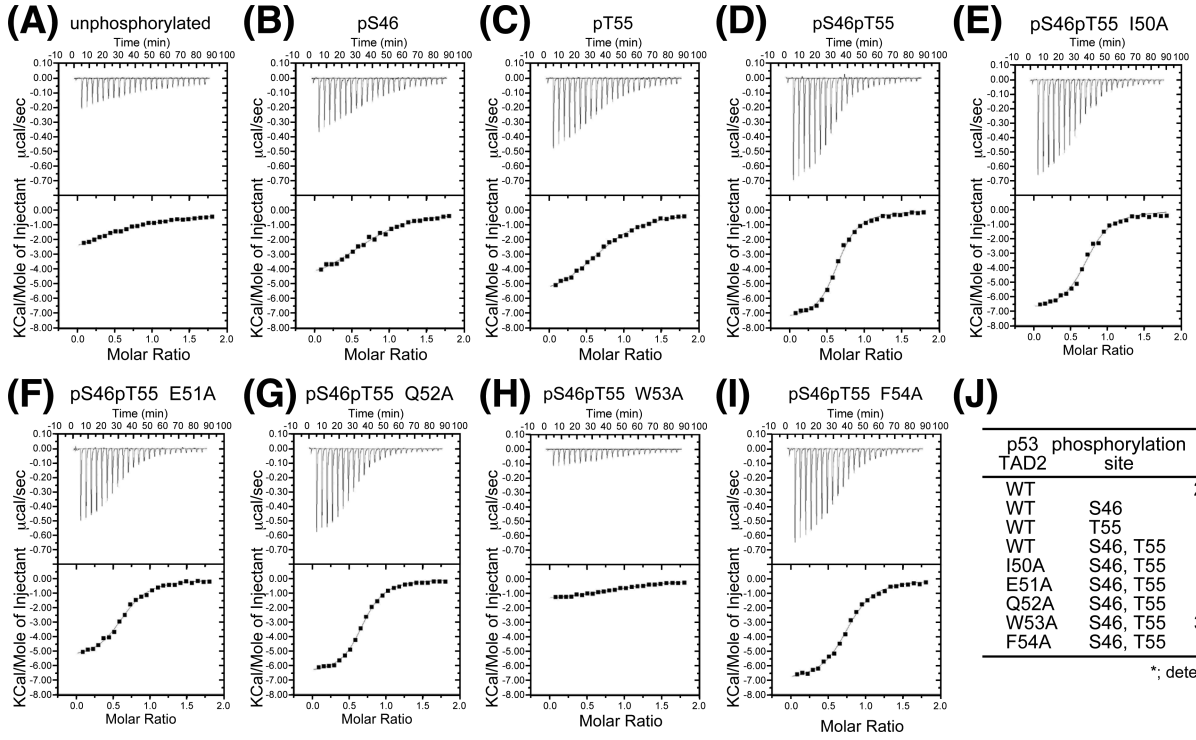

(J)

p53 TAD2	phosphorylation site	Kd (μM)
WT		24.21 ± 3.00
WT	S46	6.02 ± 0.75
WT	T55	4.85 ± 0.35
WT	S46, T55	0.96 ± 0.08
I50A	S46, T55	1.22 ± 0.15
E51A	S46, T55	1.71 ± 0.15
Q52A	S46, T55	1.02 ± 0.05
W53A	S46, T55	30.66 ± 4.78 *
F54A	S46, T55	1.35 ± 0.09

*; determined by NMR

Figure 4. Binding studies of p62 PH domain by ITC. Thermograms (upper panel) and binding isotherms (lower panel) from the calorimetric titration. Titrant: (A–D) wild-type (WT) p53 TAD2; (A) unphosphorylated, (B) S46-phosphorylated, (C) T55-phosphorylated, and (D) S46,T55-phosphorylated. (E–I) Mutants of S46,T55-phosphorylated p53 TAD2; (E) I50A, (F) E51A, (G) Q52A, (H) W53A, and (I) F54A. (J) The calculated binding dissociation constants (K_d).

consisting of seven β-strands, in which β1-β4 and β5-β7 form the first and second antiparallel β-sheets, respectively, followed by the α-helix (α1) (Figure 1). Although the isolated phosphorylated TAD2 seems to be intrinsically disordered, an extended and ordered structure was induced between residues 47–58 upon binding to the PH domain (Figure 1).

Intermolecular Interactions. The phosphorylated TAD2 runs along a positively charged path on the surface of the PH domain like an acidic string, electrostatically interacting with many lysine residues (Figure 2A and Supporting Information, Table S3). Asp48 of the phosphorylated TAD2 interacts with Lys19 in the L1 loop between strands β1 and β2 and Lys62 in the L4 loop between strands β5 and β6 of the PH domain (Figure 2B). Similarly, Asp49 of the phosphorylated TAD2 interacts with Lys60 in the L4 loop of the PH domain (Figure 2B). Glu51 of the phosphorylated TAD2 makes contact with Lys54 in the β5 strand of the PH domain, while Glu56 of the phosphorylated TAD2 interacts with Lys93 and Gln97 in the α1 helix of the PH domain (Figure 2C and Supporting Information, Figure S1). Finally, Asp57 of the phosphorylated TAD2 is in contact with Lys104 after the α1 helix of the PH domain (Figure 2C).

The structure demonstrates why the dual phosphorylation of TAD2 increases the binding to the PH domain.[11] Phosphorylated Ser46 acquires a negative potential, thereby becoming able to electrostatically interact with both Lys18 and Lys19 residues in the PH domain (Figure 2D). Analogously, phosphorylated Thr55 makes electrostatic contact with Lys54 in the PH domain (Figure 2D).

As well as the electrostatic interactions, numerous different types of interactions were observed at the interface. Ile50 of the phosphorylated TAD2 points its bulky side-chain inward, making hydrophobic contacts with the aliphatic portions of Lys60, Lys62, Gln64, and Asn76 of the PH domain (Figure 2E). The PH domain has a shallow pocket formed by Lys54, Ile55, Ser56, Gln64, Leu65, Gln66, and Asn76 (Figure 2F). The indole ring of Trp53 of the phosphorylated TAD2 is snugly inserted into the pocket and makes amino-aromatic interactions with the side-chain amino groups of Gln64, Gln66, and Asn76 of the PH domain (Figures 2E and 2F). Gln52 of the phosphorylated TAD2 takes part in the amino-aromatic interaction with Trp53 (Figure 2E). Another aromatic residue, Phe54 of the phosphorylated TAD2 goes outside of the pocket but makes hydrophobic contacts with Ile55 and Pro57 of the PH domain (Figure 2E).

Dual Phosphorylation of p53 TAD2 Enhances the Similarity to the Negatively Charged Characteristics of the N-Terminal Tail of the TFIIEα Acidic Domain. In contrast to the extended structure of the phosphorylated TAD2 of p53 (Figure 3A), the structures of unphosphorylated TAD2 in complex determined thus far are an amphipathic α-helix.[9,10,12] Even though the unphosphorylated TAD2 binds to the yeast tfb1 PH domain, it forms the amphipathic helix over residues 47–55 (Figure 3B).[11] Furthermore, in the yeast tfb1 PH domain complex the α-helix of TAD2 contacts a relatively limited surface (~800 Å^2), while in our human complex the elongated phosphorylated TAD2 string broadly contacts the surface of the second antiparallel β-sheet and α1 helix of the p62 PH domain, resulting in a much larger binding area of ~2000 Å^2.

In a previous study, we determined the structure of the complex between TFIIH p62 PH domain and TFIIEα acidic domain.[22] Like the phosphorylated TAD2 of p53, the highly acidic N-terminal tail of the TFIIEα acidic domain is disordered

dx.doi.org/10.1021/ja506351f | J. Am. Chem. Soc. 2014, 136, 14143–14152

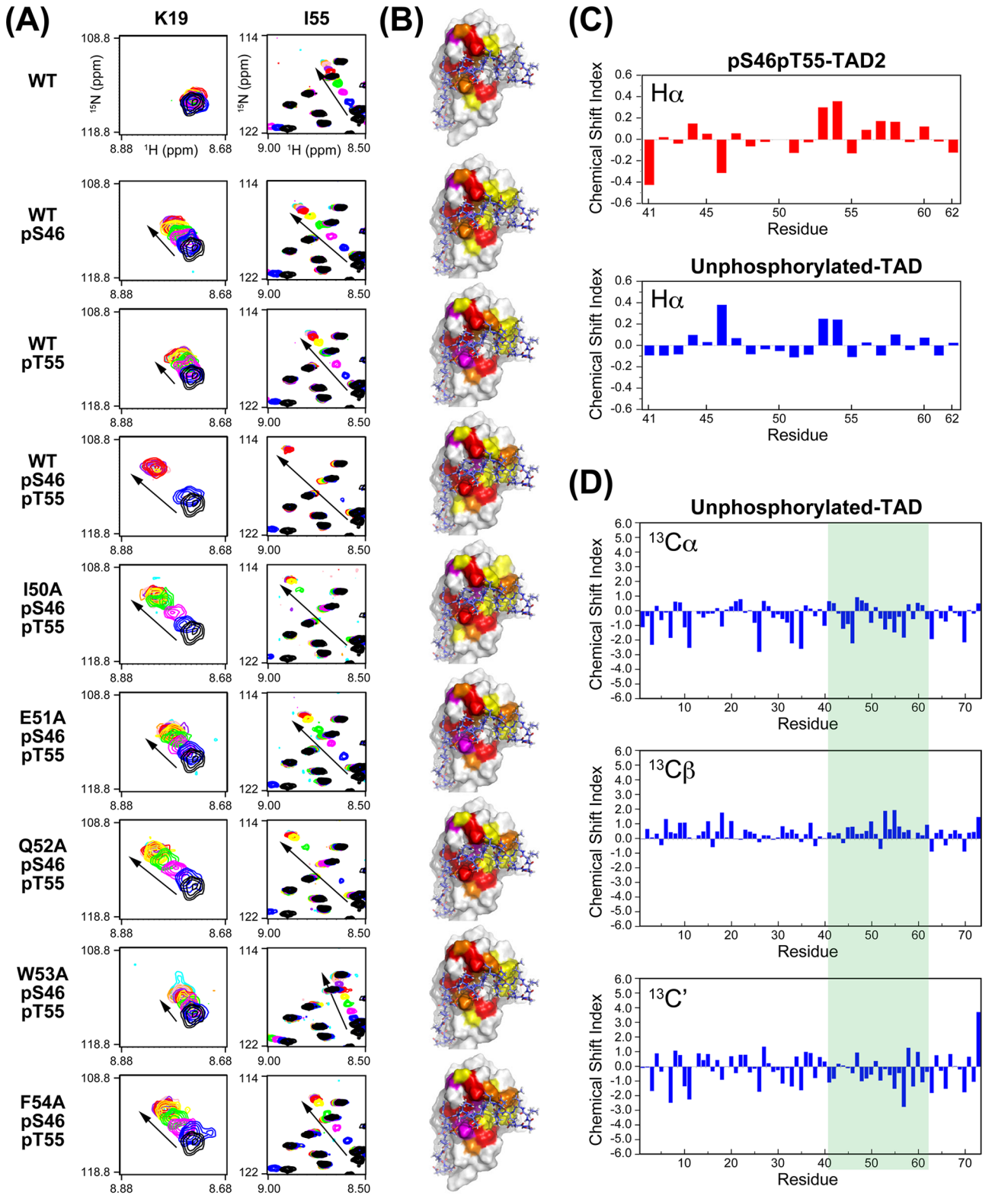

Figure 5. Binding studies of p53 TAD2 to p62 PH domain by NMR. (A) Overlays of expanded regions (Lys19 and Ile55) from 10 ^{1}H,^{15}N -HSQC spectra of p62 PH domain in the titration experiments with p53 TAD2. An arrow indicates direction of changing signal. (B) Chemical shift perturbation mapping. Residues that show more than average $\Delta\delta$ (δ_{ave}) upon addition of p53 TAD2 at a molar ratio of 1:1 are mapped onto the molecular surface of the p62 PH domain in complex with TAD2 (sticks representation). Residues are colored according to the magnitude of chemical shift change. Yellow: $2 \times \Delta\delta_{ave} > \Delta\delta \geq \Delta\delta_{ave}$. Orange: $3 \times \Delta\delta_{ave} > \Delta\delta \geq 2 \times \Delta\delta_{ave}$. Magenta: $4 \times \Delta\delta_{ave} > \Delta\delta \geq 3 \times \Delta\delta_{ave}$. Red: $\Delta\delta \geq 4 \times \Delta\delta_{ave}$. (C) Chemical shift index (CSI) of Hα for unlabeled, Ser46,Thr55-phosphorylated p53 TAD2 in complex with p62 PH domain (upper panel) and for ^{13}C/^{15}N-labeled, unphosphorylated p53 TAD (residues 1−73) in complex with p62 PH domain (TAD2 region, lower panel). (D) CSI for ^{13}C/^{15}N-labeled, unphosphorylated p53 TAD in complex with p62 PH domain: ^{13}Cα (upper panel), ^{13}Cβ (middle panel), and ^{13}C′ (lower panel). TAD2 region is highlighted in green.

dx.doi.org/10.1021/ja506351f | J. Am. Chem. Soc. 2014, 136, 14143−14152

in the unbound state.[21,22] Interestingly, the induced elongated structures of both the phosphorylated TAD2 and the N-terminal tail resemble each other even though they do not have high amino acid sequence homology (Figure 3A,C,D). In addition, the side-chain interactions are also very similar with the acidic residues of the N-terminal tail of the acidic domain making electrostatic interactions with the lysine residues of the PH domain.[22] It is noteworthy that the dual phosphorylation at Ser46 and Thr55 further increases the similarity between the phosphorylated TAD2 and the N-terminal tail of the TFIIEα acidic domain. The phosphorylated Ser46 and Thr55 in the phosphorylated TAD2 and the corresponding Asp380 and Glu389 of the TFIIEα acidic tail contact the same PH domain lysine residues, namely Lys18 and/or Lys19, and Lys54, respectively (Figure 3A vs 3C). As a result, the phosphorylated TAD2 and the TFIIEα acidic tail make electrostatic interactions with the same seven lysine residues (Lys18, Lys19, Lys54, Lys60, Lys62, Lys93, and Lys104) located along the binding path of the PH domain. The binding area of ~2000 Å^2 of the phosphorylated TAD2 complex is comparable to that of the TFIIEα acidic tail complex, ~2300 Å^2. Hence, the electrostatic interactions with the seven lysine residues are essential for the recognition of the p62 PH domain. The TFIIEα acidic tail itself has the strongest binding activity for the PH domain in the default state, while TAD2 deftly mimics such an active state via the dual phosphorylation.

Characteristics of Binding to the PH Domain. In addition to the striking similarity in the electrostatic interactions, both the phosphorylated TAD2 and the N-terminal tail of the TFIIEα acidic domain insert an aromatic ring, Trp53 of the phosphorylated TAD2 and Phe387 of the TFIIEα acidic tail into the same pocket of the PH domain, making virtually identical interactions with the pocket-forming residues[22] (Figure 3A vs 3C). The yeast tfb1 PH domain also possesses the corresponding pocket, in which it accommodates an aromatic ring of tryptophan/phenylalanine from its partner proteins.[11,25,30−33] However, the unphosphorylated TAD2 inserts Phe54 rather than Trp53 into the pocket of the yeast tfb1 PH domain (Figure 3A vs 3B). These findings indicate that the insertion of a single aromatic ring into the pocket is another critical feature for PH domain recognition.

Critical Binding Determinants. To test the validity of the two determining characteristics for p62 PH domain recognition obtained from the structural insights, we performed a mutational analysis using ITC (Figure 4). We initially examined the effect of phosphorylation of p53 TAD2 on the binding. Consistent with the present structure and the previous report,[11] the phosphorylation of TAD2 at Ser46 and Thr55 substantially enhanced the binding. In the assays performed here a single phosphorylation of Ser46 or Thr55 augmented the binding 4- or 5-fold while dual phosphorylation at Ser46 and Thr55 conferred a 25-fold increase in the strength of binding (Figure 4A−D,J).

Subsequently, we investigated the contribution of residues of the phosphorylated TAD2 to the binding by alanine substitution in a Ser46 and Thr55 phosphorylated background. Alanine substitution of Ile50, Glu51, Gln52, and Phe54 resulted in small reductions in binding; the changes in the dissociation constants (K_d) were less than 2-fold compared to wild-type (Figure 4D vs 4E−G,I,J), whereas mutation of Trp53 of the phosphorylated TAD2 led to a more than 30-fold reduction in affinity (Figure 4D vs 4H,J).

Thus, the increased electrostatic interactions produced by the phosphorylation of Ser46 and Thr55 and to a greater extent the insertion of the aromatic ring of Trp53 into the binding pocket dominate the binding of the phosphorylated TAD2 to the p62 PH domain.

Binding Modes of Unphosphorylated TAD2 and TAD2 Mutants. Human p53 TAD2 bound to human p62 PH domain as a string-like conformation is doubly phosphorylated, but human p53 TAD2 when bound to yeast tfb1 PH domain as an amphipathic helix is unphosphorylated. Thus, the question arises whether the unphosphorylated human p53 TAD2 folds into a similar amphipathic α-helix upon binding to human p62 PH domain. If so, significant changes in the contact area on the p62 PH domain would arise upon the dephosphorylation of p53 TAD2. We therefore performed NMR titration experiments for ^{15}N-labeled p62 PH domain by adding the unphosphorylated TAD2 and TAD2 singly phosphorylated at Ser46 or Thr55 (Figure 5A and Supporting Information, Figure S2). By adding these TAD2 derivatives, several signals from specific residues of the PH domain underwent fast exchange on the NMR time scale because of the weak binding of these TAD2 derivatives (Figure 5A). By adding TAD2 doubly phosphorylated at Ser46 and Thr55, these signals underwent medium to slow exchange because of the strong binding. It is apparent that the chemical shift changes of these signals increased proportionally to the degrees of phosphorylation. The degrees of these chemical shift changes observed in the NMR titration experiments could reflect the binding activities of p53 derivatives to the p62 PH domain, and this is essentially supported by ITC experiments (Figure 4). Importantly, the profiles of the chemical shift perturbation upon addition of p53 derivatives strongly resemble each other, regardless of the phosphorylation states (Figure S2). The deduced contact areas on the PH domain were essentially identical for the binding of all TAD2 derivatives (Figure 5B).

In the same way we observed the NMR signal changes of the PH domain when titrated with the alanine mutants, I50A, E51A, Q52A, W53A, and F54A of TAD2 phosphorylated at Ser46 and Thr55. Except for W53A, all mutants exhibited large chemical shift changes to a similar extent as the doubly phosphorylated wild type (WT pS46pT55) (Figure 5A and Figure S2). Like WT pS46pT55, I50A and Q52A underwent medium to slow exchange on the NMR time scale in the signal of Ile55. In contrast, W53A showed relatively small chemical shift changes in a similar manner to the unphosphorylated WT. Although large differences in the chemical shift changes were observed between W53A and other alanine mutants, their estimated contact surfaces were essentially identical to each other and to those of the unphosphorylated and phosphorylated WT (Figure S2 and Figure 5B). This means that Trp53 plays a critical role in strengthening the binding but does not significantly alter the contact area.

To obtain more compelling data on the conformation of unphosphorylated TAD2 bound to the PH domain, we examined the secondary structure using a chemical shift index (CSI) method. For this, we prepared ^{13}C/^{15}N-labeled TAD (residues 1−73) from an *E. coli* expression system and examined its binding ability by NMR as shown in Supporting Information, Figure S3. The TAD2 region in the TAD is greatly affected by binding to the PH domain. The CSI of Hα for the unphosphorylated TAD2 in TAD in complex with the PH domain was similar to that of the elongated diphosphorylated TAD2 (Figure 5C and Figure S3). The CSI of ^{13}Cα, ^{13}Cβ, and

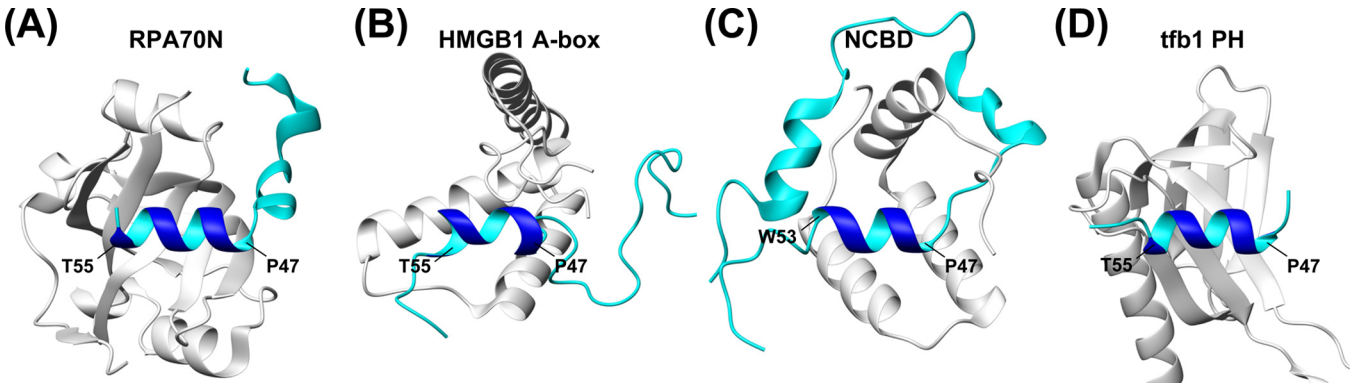

Figure 6. Amphipathic helix structures of p53 unphosphorylated TAD2 in complex with binding partners. (A) Complex with the N-terminal domain of the RPA70 subunit of replication protein A (RPA70N) (PDB code 2B3G). (B) Complex with the A box of high-mobility group B1 (HMGB1 A-box) (PDB code 2LY4). (C) Complex with the nuclear receptor co-activator binding domain of CBP (NCBD) (PDB code 2L14). (D) Complex with the PH domain of tfb1 (PDB code 2GS0). p53 and its binding partners are shown in cyan and white, respectively. The amphipathic helix in p53 TAD2 is indicated in blue/cyan.

$^{13}C'$ also indicated that the unphosphorylated TAD2 does not form a helix, but rather takes up an extended structure (Figure 5D). These results strongly rule out the possibility of amphipathic helix formation by the unphosphorylated TAD2 upon binding to the p62 PH domain; the unphosphorylated TAD2 is likely to bind to the p62 PH domain in a string-like conformation similar to the binding mode of the doubly phosphorylated TAD2.

DISCUSSION

In the present study, we have investigated the interaction between two different types of hub domains, a coupled folding and binding type hub domain, the phosphorylated TAD2 of p53,[59] and an uncoupled rather rigid hub domain, the p62 PH domain of TFIIH and revealed how such a pliable TAD2 optimally binds to the rigid p62 PH domain. First we had assumed that the TAD2 would form a canonical amphipathic α-helix, because the binding-coupled amphipathic α-helix formation is commonly used to capture its various partners.[9,10,12−14] All available structures of unphosphorylated TAD2 in complex show that it contains an amphipathic α-helix (Figure 6). The residues Pro47-Thr55 of TAD2 form the amphipathic helix in complex with the N-terminal domain of the RPA70 subunit of replication protein A (RPA70N)[10] (Figure 6A) and the A box of high-mobility group B1 (HMGB1 A-box)[12] (Figure 6B). Similarly, residues Pro47-Trp53 of TAD2 form the amphipathic helix in complex with the nuclear receptor co-activator binding domain of CBP (NCBD)[9] (Figure 6C). In addition the PH domain of tfb1, the budding yeast homologue of p62 is no exception; the unphosphorylated TAD2 induces a nine residue amphipathic α-helix over residues 47−55 upon binding to the PH domain (Figures 6D and 3B).[11] Unexpectedly, however, TAD2 phosphorylated at Ser46 and Thr55 showed previously unknown conformational malleability; i.e., the phosphorylated and probably the unphosphorylated TAD2 do not form an amphipathic α-helix but rather an elongated string-like structure on the human p62 PH domain. The structural comparison with the complex of TFIIEα acidic domain[22] in combination with the mutational analyses enabled us to understand why the TAD2 uses the unusual binding mode. These define the two critical characteristics for the recognition of the p62 PH domain. The first feature is the extensive electrostatic interactions with seven lysine residues of the p62 PH domain, three of which are not conserved in the budding yeast homologue, tfb1.[58] Remarkably, the phosphorylated TAD2 strictly adheres to this feature by dual phosphorylation at Ser46 and Thr55. The second feature is the insertion of an aromatic ring into the binding pocket. The first feature allows room for the degrees of freedom of backbone and side chains of the negatively charged and neighboring residues, and thereby offers the malleability to the partners of the p62 PH domain. The second feature is strict in its requirements and thus directly contributes to the specificity of binding. An amphipathic α-helix structure is unlikely to exhibit these features. To faithfully obey the two features, it is necessary for the phosphorylated TAD2 to take up an extended conformation rather than forming the amphipathic α-helix.

One of the most important characteristics of p53 is its gene selectivity. Many studies have indicated that an array of post-translational modifications on p53 play crucial roles in gene selection.[35,36] Phosphorylation is of particular importance. Notably, a number of studies have reported that the phosphorylation of Ser46 in the TAD is involved in the activation of the apoptosis activity of p53. In response to repairable DNA damage p53 is phosphorylated at Ser15 and Ser20 and activates cell cycle arrest genes and in more severe damage, the phosphorylation of Ser46 occurs and p53 activates proapoptotic genes.[46] A genome-wide study showed that overall DNA-binding patterns of p53 are similar upon cell cycle arrest-inducing Actinomycin D treatment and apoptosis-inducing Etoposide treatment, whereas the extent of phosphorylation of Ser46 is considerably higher upon Etoposide treatment.[60] In contrast, the phosphorylation of Thr55 has been shown to be involved in p53 inactivation. Thr55-phosphorylation by TAF1 results in MDM2-mediated p53 degradation and leads to a decrease in cell G1 arrest.[47] The phosphorylation of this residue also induces the association of p53 with the nuclear export factor CRM1 and leads to p53 nuclear export.[48] A recent study indicated that the phosphorylation of Thr55 by TAF1 in an ATP-dependent manner leads to dissociation of p53 from promoters such as *p21* and the dissociation results in inactivation of p53 transcription after recovery from DNA damage.[61] Hence, the roles of the phosphorylation at Ser46 and at Thr55 appear functionally irrelevant. However, here we structurally demonstrate that the combinatorial phosphorylation of Ser46 and Thr55 is able to enhance the binding of TAD2 to the PH domain of p62 25-fold

dx.doi.org/10.1021/ja506351f | J. Am. Chem. Soc. 2014, 136, 14143−14152

by making additional electrostatic interactions. Active p53 is a homotetramer, so that the enhancement of affinity observed here may be amplified *in vivo*. In the interactions between the p53 TAD and the co-activators, p300 and CBP, the affinities were increased more by the multiple phosphorylation than by each single phosphorylation.[39−42] *In vivo* studies using p53 knock-in mouse models indicated that impairment of p53-dependent apoptosis was more severe in p53 S18A and S23A (S15A and S20A in human) double-mutant mice than in p53 S18A or p53 S23A single-mutant mice.[62−64] Thus, the combinatorial phosphorylation of p53 TAD seems to be important for the interactions with these co-activators.

Depending on the kinds and degree of stresses and the cell types, post-translational modifications occur on p53 and its specific modification pattern could modulate interactions among players in gene regulation including chromatin related factors and ultimately provide selective context for expression of desired genes.[65] Considering the diverse responses of p53 to stress, the combinatorial phosphorylation of Ser46 and Thr55 in p53, which increases the affinity for the basal transcriptional machinery, may participate in the context selectivity for expression of certain specific genes. It will therefore be of great interest to see the phosphorylation states of Ser46 and Thr55 when cells are confronted with different stresses.

Structural studies on the recognition mechanisms of hub domains are of paramount importance for studying complex networks. In particular, research into the networks involved in p53 will be extremely helpful for designing cancer therapeutic drugs.

■ ASSOCIATED CONTENT

Supporting Information

Three figures and three tables. This material is available free of charge via the Internet at http://pubs.acs.org.

■ AUTHOR INFORMATION

Corresponding Author

nisimura@tsurumi.yokohama-cu.ac.jp

Notes

The authors declare no competing financial interest.

■ ACKNOWLEDGMENTS

The authors thank Prof. Y. Ohkuma for kindly providing the expression vector for the p53 TAD. This work was supported by the Grants-in-Aid for Scientific Research (M.O. and Y.N.), the Grants-in-Aid for Scientific Research on Innovative Areas (Y.N.), and the Platform for Drug Discovery, Informatics, and Structural Life Science (Y.N.) from the Ministry of Education, Culture, Sports, Science and Technology, Japan.

■ REFERENCES

(1) Ko, L. J.; Prives, C. *Genes Dev.* **1996**, *10*, 1054−1072.
(2) Levine, A. J. *Cell* **1997**, *88*, 323−331.
(3) Vogelstein, B.; Lane, D.; Levine, A. J. *Nature* **2000**, *408*, 307−310.
(4) Vousden, K. H.; Lane, D. P. *Nat. Rev. Mol. Cell. Biol.* **2007**, *8*, 275−283.
(5) Lee, H.; Mok, K. H.; Muhandiram, R.; Park, K. H.; Suk, J. E.; Kim, D. H.; Chang, J.; Sung, Y. C.; Choi, K. Y.; Han, K. H. *J. Biol. Chem.* **2000**, *275*, 29426−29432.
(6) Kussie, P. H.; Gorina, S.; Marechal, V.; Elenbaas, B.; Moreau, J.; Levine, A. J.; Pavletich, N. P. *Science* **1996**, *274*, 948−953.
(7) Popowicz, G. M.; Czarna, A.; Holak, T. A. *Cell Cycle* **2008**, *7*, 2441−2443.
(8) Feng, H.; Jenkins, L. M.; Durell, S. R.; Hayashi, R.; Mazur, S. J.; Cherry, S.; Tropea, J. E.; Miller, M.; Wlodawer, A.; Appella, E.; Bai, Y. *Structure* **2009**, *17*, 202−210.
(9) Lee, C. W.; Martinez-Yamout, M. A.; Dyson, H. J.; Wright, P. E. *Biochemistry* **2010**, *49*, 9964−9971.
(10) Bochkareva, E.; Kaustov, L.; Ayed, A.; Yi, G. S.; Lu, Y.; Pineda-Lucena, A.; Liao, J. C.; Okorokov, A. L.; Milner, J.; Arrowsmith, C. H.; Bochkarev, A. *Proc. Natl. Acad. Sci. U.S.A.* **2005**, *102*, 15412−15417.
(11) Di Lello, P.; Jenkins, L. M.; Jones, T. N.; Nguyen, B. D.; Hara, T.; Yamaguchi, H.; Dikeakos, J. D.; Appella, E.; Legault, P.; Omichinski, J. G. *Mol. Cell* **2006**, *22*, 731−740.
(12) Rowell, J. P.; Simpson, K. L.; Stott, K.; Watson, M.; Thomas, J. O. *Structure* **2012**, *20*, 2014−2024.
(13) Rajagopalan, S.; Andreeva, A.; Teufel, D. P.; Freund, S. M.; Fersht, A. R. *J. Biol. Chem.* **2009**, *284*, 21728−21737.
(14) Ha, J. H.; Shin, J. S.; Yoon, M. K.; Lee, M. S.; He, F.; Bae, K. H.; Yoon, H. S.; Lee, C. K.; Park, S. G.; Muto, Y.; Chi, S. W. *J. Biol. Chem.* **2013**, *288*, 7387−7398.
(15) Vassilev, L. T.; Vu, B. T.; Graves, B.; Carvajal, D.; Podlaski, F.; Filipovic, Z.; Kong, N.; Kammlott, U.; Lukacs, C.; Klein, C.; Fotouhi, N.; Liu, E. A. *Science* **2004**, *303*, 844−848.
(16) Ding, K.; Lu, Y.; Nikolovska-Coleska, Z.; Qiu, S.; Ding, Y.; Gao, W.; Stuckey, J.; Krajewski, K.; Roller, P. P.; Tomita, Y.; Parrish, D. A.; Deschamps, J. R.; Wang, S. *J. Am. Chem. Soc.* **2005**, *127*, 10130−10131.
(17) Grasberger, B. L.; Lu, T.; Schubert, C.; Parks, D. J.; Carver, T. E.; Koblish, H. K.; Cummings, M. D.; LaFrance, L. V.; Milkiewicz, K. L.; Calvo, R. R.; Maguire, D.; Lattanze, J.; Franks, C. F.; Zhao, S.; Ramachandren, K.; Bylebyl, G. R.; Zhang, M.; Manthey, C. L.; Petrella, E. C.; Pantoliano, M. W.; Deckman, I. C.; Spurlino, J. C.; Maroney, A. C.; Tomczuk, B. E.; Molloy, C. J.; Bone, R. F. *J. Med. Chem.* **2005**, *48*, 909−912.
(18) Reed, D.; Shen, Y.; Shelat, A. A.; Arnold, L. A.; Ferreira, A. M.; Zhu, F.; Mills, N.; Smithson, D. C.; Regni, C. A.; Bashford, D.; Cicero, S. A.; Schulman, B. A.; Jochemsen, A. G.; Guy, R. K.; Dyer, M. A. *J. Biol. Chem.* **2010**, *285*, 10786−10796.
(19) Bernal, F.; Tyler, A. F.; Korsmeyer, S. J.; Walensky, L. D.; Verdine, G. L. *J. Am. Chem. Soc.* **2007**, *129*, 2456−2457.
(20) Xiao, H.; Pearson, A.; Coulombe, B.; Truant, R.; Zhang, S.; Regier, J. L.; Triezenberg, S. J.; Reinberg, D.; Flores, O.; Ingles, C. J. *Mol. Cell. Biol.* **1994**, *14*, 7013−7024.
(21) Di Lello, P.; Miller Jenkins, L. M.; Mas, C.; Langlois, C.; Malitskaya, E.; Fradet-Turcotte, A.; Archambault, J.; Legault, P.; Omichinski, J. G. *Proc. Natl. Acad. Sci. U.S.A.* **2008**, *105*, 106−111.
(22) Okuda, M.; Tanaka, A.; Satoh, M.; Mizuta, S.; Takazawa, M.; Ohkuma, Y.; Nishimura, Y. *EMBO J.* **2008**, *27*, 1161−1171.
(23) Pearson, A.; Greenblatt, J. *Oncogene* **1997**, *15*, 2643−2658.
(24) Chen, D.; Riedl, T.; Washbrook, E.; Pace, P. E.; Coombes, R. C.; Egly, J. M.; Ali, S. *Mol. Cell* **2000**, *6*, 127−137.
(25) Mas, C.; Lussier-Price, M.; Soni, S.; Morse, T.; Arseneault, G.; Di Lello, P.; Lafrance-Vanasse, J.; Bieker, J. J.; Omichinski, J. G. *Proc. Natl. Acad. Sci. U.S.A.* **2011**, *108*, 10484−10489.
(26) Tong, X.; Drapkin, R.; Reinberg, D.; Kieff, E. *Proc. Natl. Acad. Sci. U.S.A.* **1995**, *92*, 3259−3263.
(27) Yokoi, M.; Masutani, C.; Maekawa, T.; Sugasawa, K.; Ohkuma, Y.; Hanaoka, F. *J. Biol. Chem.* **2000**, *275*, 9870−9875.
(28) Iyer, N.; Reagan, M. S.; Wu, K. J.; Canagarajah, B.; Friedberg, E. C. *Biochemistry* **1996**, *35*, 2157−2167.
(29) Morin, G.; Fradet-Turcotte, A.; Di Lello, P.; Bergeron-Labrecque, F.; Omichinski, J. G.; Archambault, J. *J. Virol.* **2011**, *85*, 5287−5300.
(30) Langlois, C.; Mas, C.; Di Lello, P.; Jenkins, L. M.; Legault, P.; Omichinski, J. G. *J. Am. Chem. Soc.* **2008**, *130*, 10596−10604.
(31) Lafrance-Vanasse, J.; Arseneault, G.; Cappadocia, L.; Chen, H. T.; Legault, P.; Omichinski, J. G. *Nucleic Acids Res.* **2012**, *40*, 5739−5750.

(32) Lafrance-Vanasse, J.; Arseneault, G.; Cappadocia, L.; Legault, P.; Omichinski, J. G. *Nucleic Acids Res.* **2013**, *41*, 2736−2745.
(33) Chabot, P. R.; Raiola, L.; Lussier-Price, M.; Morse, T.; Arseneault, G.; Archambault, J.; Omichinski, J. G. *PLoS Pathog.* **2014**, *10*, No. e1004042.
(34) Di Lello, P.; Nguyen, B. D.; Jones, T. N.; Potempa, K.; Kobor, M. S.; Legault, P.; Omichinski, J. G. *Biochemistry* **2005**, *44*, 7678−7686.
(35) Bode, A. M.; Dong, Z. *Nat. Rev. Cancer* **2004**, *4*, 793−805.
(36) Kruse, J. P.; Gu, W. *Cell* **2009**, *137*, 609−622.
(37) Jenkins, L. M.; Durell, S. R.; Mazur, S. J.; Appella, E. *Carcinogenesis* **2012**, *33*, 1441−1449.
(38) Sakaguchi, K.; Saito, S.; Higashimoto, Y.; Roy, S.; Anderson, C. W.; Appella, E. *J. Biol. Chem.* **2000**, *275*, 9278−9283.
(39) Teufel, D. P.; Bycroft, M.; Fersht, A. R. *Oncogene* **2009**, *28*, 2112−2118.
(40) Polley, S.; Guha, S.; Roy, N. S.; Kar, S.; Sakaguchi, K.; Chuman, Y.; Swaminathan, V.; Kundu, T.; Roy, S. *J. Mol. Biol.* **2008**, *376*, 8−12.
(41) Ferreon, J. C.; Lee, C. W.; Arai, M.; Martinez-Yamout, M. A.; Dyson, H. J.; Wright, P. E. *Proc. Natl. Acad. Sci. U.S.A.* **2009**, *106*, 6591−6596.
(42) Lee, C. W.; Ferreon, J. C.; Ferreon, A. C.; Arai, M.; Wright, P. E. *Proc. Natl. Acad. Sci. U.S.A.* **2010**, *107*, 19290−19295.
(43) Higashimoto, Y.; Saito, S.; Tong, X. H.; Hong, A.; Sakaguchi, K.; Appella, E.; Anderson, C. W. *J. Biol. Chem.* **2000**, *275*, 23199−23203.
(44) Saito, S.; Yamaguchi, H.; Higashimoto, Y.; Chao, C.; Xu, Y.; Fornace, A. J., Jr.; Appella, E.; Anderson, C. W. *J. Biol. Chem.* **2003**, *278*, 37536−37544.
(45) Bulavin, D. V.; Saito, S.; Hollander, M. C.; Sakaguchi, K.; Anderson, C. W.; Appella, E.; Fornace, A. J., Jr. *EMBO J.* **1999**, *18*, 6845−6854.
(46) Oda, K.; Arakawa, H.; Tanaka, T.; Matsuda, K.; Tanikawa, C.; Mori, T.; Nishimori, H.; Tamai, K.; Tokino, T.; Nakamura, Y.; Taya, Y. *Cell* **2000**, *102*, 849−862.
(47) Li, H. H.; Li, A. G.; Sheppard, H. M.; Liu, X. *Mol. Cell* **2004**, *13*, 867−878.
(48) Cai, X.; Liu, X. *Proc. Natl. Acad. Sci. U.S.A.* **2008**, *105*, 16958−16963.
(49) Cavanagh, J.; Fairbroher, W. J.; Palmer, A. G., III; Skelton, N. J. *Protein NMR spectroscopy*; Academic Press: San Diego, CA, 1996.
(50) Delaglio, F.; Grzesiek, S.; Vuister, G. W.; Zhu, G.; Pfeifer, J.; Bax, A. *J. Biomol. NMR* **1995**, *6*, 277−293.
(51) Johnson, B. A.; Blevins, R. A. *J. Biomol. NMR* **1994**, *4*, 603−614.
(52) Cornilescu, G.; Delaglio, F.; Bax, A. *J. Biomol. NMR* **1999**, *13*, 289−302.
(53) Brünger, A. T. *X-PLOR Version 3.1: A system for X-ray crystallography and NMR*; Yale University Press: New Haven, CT, 1993.
(54) Schwieters, C. D.; Kuszewski, J. J.; Tjandra, N.; Clore, G. M. *J. Magn. Reson.* **2003**, *160*, 65−73.
(55) Linge, J. P.; Williams, M. A.; Spronk, C. A.; Bonvin, A. M.; Nilges, M. *Proteins* **2003**, *50*, 496−506.
(56) Laskowski, R. A.; Rullmann, J. A. C.; MacArthur, M. W.; Kaptein, R.; Thornton, J. M. *J. Biomol. NMR* **1996**, *8*, 477−486.
(57) Koradi, R.; Billeter, M.; Wüthrich, K. *J. Mol. Graph.* **1996**, *14*, 51−55.
(58) Gervais, V.; Lamour, V.; Jawhari, A.; Frindel, F.; Wasielewski, E.; Dubaele, S.; Egly, J. M.; Thierry, J. C.; Kieffer, B.; Poterszman, A. *Nat. Struct. Mol. Biol.* **2004**, *11*, 616−622.
(59) Wright, P. E.; Dyson, H. J. *J. Mol. Biol.* **1999**, *293*, 321−331.
(60) Smeenk, L.; van Heeringen, S. J.; Koeppel, M.; Gilbert, B.; Janssen-Megens, E.; Stunnenberg, H. G.; Lohrum, M. *PLoS One* **2011**, *6*, No. e17574.
(61) Wu, Y.; Lin, J. C.; Piluso, L. G.; Dhahbi, J. M.; Bobadilla, S.; Spindler, S. R.; Liu, X. *Mol. Cell* **2014**, *53*, 63−74.
(62) MacPherson, D.; Kim, J.; Kim, T.; Rhee, B. K.; Van Oostrom, C. T.; DiTullio, R. A.; Venere, M.; Halazonetis, T. D.; Bronson, R.; De Vries, A.; Fleming, M.; Jacks, T. *EMBO J.* **2004**, *23*, 3689−3699.
(63) Sluss, H. K.; Armata, H.; Gallant, J.; Jones, S. N. *Mol. Cell. Biol.* **2004**, *24*, 976−984.
(64) Chao, C.; Herr, D.; Chun, J.; Xu, Y. *EMBO J.* **2006**, *25*, 2615−2622.
(65) Espinosa, J. M. *Oncogene* **2008**, *27*, 4013−4023.

NOTE ADDED AFTER ASAP PUBLICATION

The PDB code in the Figure 3 (A) caption was corrected on October 8, 2014.